FISEVIER

Contents lists available at ScienceDirect

Science of the Total Environment

journal homepage: www.elsevier.com/locate/scitotenv



Contrasting ecosystem responses to climatic events and human activity revealed by a sedimentary record from Lake Yilong, southwestern China



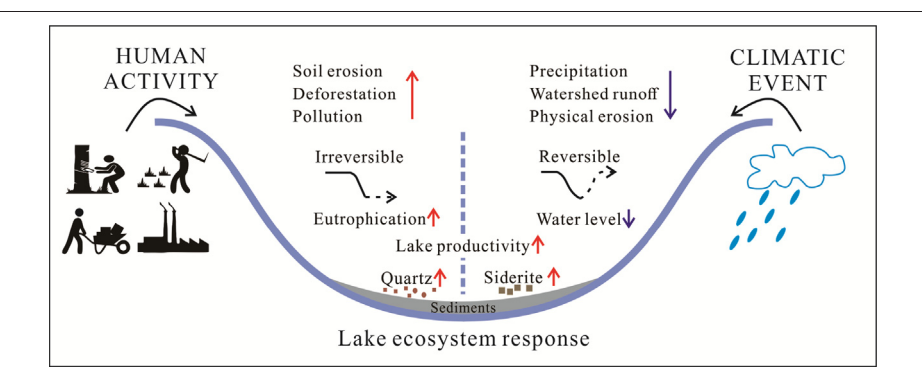
Zijie Yuan ^a, Duo Wu ^{a,*}, Lili Niu ^a, Xuyi Ma ^a, Youmo Li ^a, Aubrey L. Hillman ^b, Mark B. Abbott ^c, Aifeng Zhou ^a

- a College of Earth and Environmental Sciences, MOE Key Laboratory of Western China's Environmental Systems, Lanzhou University, Lanzhou 730000, China
- b Department of Atmospheric and Environmental Sciences, University at Albany, State University of New York, Albany 12222, USA
- ^c Department of Geology and Environmental Science, University of Pittsburgh, Pittsburgh 15260, USA

HIGHLIGHTS

- Lacustrine record of environmental change over the last 12 ka from southwestern China
- Ecosystem was impacted by the 9.3 ka climate event and by human activity after 1.5 ka.
- Lake ecosystem was resilient in the face of a climatic perturbation.
- Human activities had an irreversible impact on the lake ecosystem.
- Greater impact of human activity on the lake ecosystem compared to climate change

GRAPHICAL ABSTRACT



ARTICLE INFO

Article history: Received 25 January 2021 Received in revised form 27 March 2021 Accepted 30 March 2021 Available online xxxx

Editor: Fernando A.L. Pacheco

Keywords: Indian Summer Monsoon Abrupt climatic event Human impacts Holocene Lake Yilong Ecosystem response

ABSTRACT

Global climate change and human activities have significantly impacted lake ecosystems at an accelerating rate in recent decades, but the differences between the responses of lake ecosystems to these two stressors remain unclear. Thus an improved understanding of the long-term influences of climatic and anthropogenic disturbances is necessary for the management of lake ecosystems. In order to address these issues, a sedimentary record was obtained from Lake Yilong in Yunnan Province in southwestern China, where the climate and natural environment are dominated by the Indian Summer Monsoon and there is a long history of human occupation and intensive human activity. The chronology is based on AMS ¹⁴C dates from 13 samples of plant macrofossils and charcoal, which show that the record spans the last ~12,000 yr. Geochemical indices were used to reconstruct hydroclimatic variations and lake ecosystem responses. The results indicate that a cold and humid climate prevailed from the late Pleistocene to the beginning of the Holocene, which was interrupted by an abrupt decrease in precipitation during 9.7-8.7 ka (1 ka = 1000 cal yr BP, corresponding to the 9.3 ka event). A persistent drying trend occurred during the middle and late Holocene, and there was an increase in the intensity of human activity during the past 1500 years. A comparison of the effects of a natural climatic event and human disturbance reveals contrasting lake ecosystem responses. The lake ecosystem was resilient to the 9.3 ka event and subsequently recovered; however, long-term human activity in the watershed, including deforestation and cultivation, reduced the stability of the lake ecosystem and positive feedback effects were strengthened, leading to the deviation of the system far from its previous stable state. It is concluded that, compared to climate change, human activities have had a much more serious impact on lake ecosystem.

© 2021 Elsevier B.V. All rights reserved.

* Corresponding author. E-mail address: dwu@lzu.edu.cn (D. Wu).

1. Introduction

Humans are altering the planet at an accelerating rate, with a consequent rapid increase in environmental problems including pollution, biodiversity loss, and the decrease of ecosystem services (Waters et al., 2016). In order to improve our understanding of the magnitude and timing of past human impacts on the natural environment, it is necessary to conduct investigations on a long timescale. It has been shown that the modification of vegetated landscapes in southern China probably began at ~6000 cal yr BP (Cheng et al., 2018), and that on the global scale, measurable human impacts on soil erosion resulting from agriculture may date to at least 4000 cal yr BP (Jenny et al., 2019). Notably, during the historical period of the past 2000 years, human activities have dominated dust storm activity in northern China (Chen et al., 2020).

It is widely accepted that lacustrine deposits can provide highly-resolved paleoenvironmental time series which can help elucidate the operation and impacts of complex socio-ecological systems at the regional scale (Dearing, 2013). Lake sediments not only provide a record of anthropogenic impacts on landscapes, but they also document changes in lake ecosystems under the long-term influences of human activity in the watershed. Human activity has serious impacts on the structure and functioning of ecosystems, as well as on ecosystem services (Sun et al., 2020). Among the various types of human activity, land use change exerts some of the most profound impacts on ecosystems (Wen et al., 2020). Thus a study comparing landscape changes and lake ecosystem responses can provide an improved understanding of anthropogenic influences on the natural environment.

Natural climate change has also significantly impacted lake ecosystems. A study of sedimentary carbon isotope records from Lake Tanganyika in East Africa indicated that global climate change has caused a decrease in lake primary productivity, as well as in aquatic ecosystem functions and services (O'Reilly et al., 2003). It was also concluded that the impact of global change on the lake ecosystem was greater than that of local anthropogenic activity (O'Reilly et al., 2003). However, a study of Lake Superior in North America indicated that recent anthropogenic climatic warming has caused a rapid increase in lake primary productivity (O'Beirne et al., 2017). Therefore, the relative impacts of climate change and human activity on lake ecosystems can vary and in some cases they are unclear. Such uncertainties hinder an accurate assessment of the effects of climate change on water resources management (Kansoh et al., 2020) and agricultural development (Fenu and Maridina, 2020), as well as on projections of the impact of future climate change on various types of runoff (Ekwueme and Agunwamba, 2020; Han et al., 2020; Javadinejad et al., 2020).

As a main component of the tropical monsoonal system (Goswami et al., 2003), the Indian Summer Monsoon (ISM) is a three-dimensional planetary circulation system produced by the northward movement of the Intertropical Convergence Zone (ITCZ) and is characterized by pronounced spatiotemporal variations (Tomas and Webster, 1997; An et al., 2015). The ISM is of great significance for the socio-economic and cultural development of the Indian subcontinent, southeastern Asia and southwestern China, as a result of variations in ISM precipitation (Webster et al., 1998; An et al., 2011); and it also plays an important role in maintaining an ecological balance and the biodiversity of ecosystems in its region of influence (Wang et al., 2005a; Govil and Divakar Naidu, 2011; Cook et al., 2013; Wu et al., 2015b). On a longer timescale, it has been found that abrupt declines in the ISM resulted in episodes of a lowered lake level at Lake Xingyun in Yunnan during the last glacial, and a corresponding increase in the concentration of Pediastrum (a type of alga) in the lake water (Wu et al., 2015b). A robust understanding of the variability of the ISM since the last deglaciation, based on reliable and high-resolution paleoclimatic reconstructions, is needed for the region dominated by the ISM, so that the impacts of abrupt climate changes on its terrestrial ecosystems can be effectively assessed.

The Yunnan Plateau, in southwestern China, is located in the region influenced by the ISM. There are numerous lakes of tectonic origin on the plateau and they are valuable archives for reconstructing past climate changes. Yunnan has a long history of human occupation and is rich in Paleolithic, Neolithic and Bronze Age archaeological sites, as well as in archaeological sites dating to the historical period (Li, 2004); thus it is well suited studying past humanenvironment interactions. Several studies have been conducted on lakes in Yunnan in order to reconstruct changes in paleoclimatic and paleoenvironmental conditions on different timescales, as well in past human activities (Shen et al., 2005; Dearing et al., 2008; Jones et al., 2012; Song et al., 2012; Zhang et al., 2012; Wu et al., 2015a, 2018; Liu and Wang, 2016; Hillman et al., 2016, 2020; Xiao et al., 2018). For example, it has been shown that anthropogenic deforestation in the Lake Erhai region occurred after the middle Holocene (Shen et al., 2005; Dearing et al., 2008), while more significant human influences on the natural environment of the Yunnan Plateau occurred in the late Holocene, or even in recent decades (Wu et al., 2015a; Hillman et al., 2016; Wang et al., 2016). However, most of these studies have focused on the timing and intensity of anthropogenic influences against a background of long-term climate change, and a more detailed understanding of the impact of human activities on lake ecosystems in the region is needed. Specifically, a comparison of the influence of natural climatic events and anthropogenic impacts on lake ecosystems in Yunnan may help us to better understand how human activities have influenced their natural trajectory. In order to address this issue, reliable proxy records of landscape and lake ecosystem changes are needed, which can enable a comparison of the histories of the ISM and regional human activity.

As one of the most eutrophic lakes in China, the ecosystem of Lake Yilong in the Yunnan Plateau has been gradually degraded due to the long-term impact of human activities (Du et al., 2019; Cheng et al., 2020a; Zhao et al., 2020). Thus, the lake is well situated for addressing questions regarding long-term environmental change and lake ecosystem variations associated with human disturbance. The main objective of the study was to compare how and to what extent the lake ecosystem responded to natural climatic events and human activity. Human activities would be expected to cause an increase the rate of soil erosion within the terrestrial catchment and water pollution within the lake, as well as a decrease in ecosystem functioning. It is hypothesized that unlike the influence of natural climate events, the effects of human activities had a rapid, intensive and irreversible impact on the lake ecosystem. To test this hypothesis, high-resolution measurements of physical and geochemical proxies from a sediment core from Lake Yilong were conducted. Based on records of sediment composition, the concentrations of organic carbon and nitrogen, the oxygen and carbon isotopic composition of authigenic carbonate, and element concentrations, environmental and climatic changes at Lake Yilong watershed during the past ~12,000 years were reconstructed. Finally, a comparison of the relative impacts of a natural climatic event and human activity on the lake ecosystem was made.

2. Materials and methods

2.1. Regional setting

Lake Yilong (23°38′ to 23°42′N and 102°30′ to 102°38′E) is a hydrologically open, shallow lake in the southern part of Yunnan Province in southwestern China (Fig. 1a). The lake surface lies at an altitude of 1412 m above mean sea level, and the average depth is 2.4 m (Wang and Dou, 1998). The area of the Lake Yilong watershed is ~305 km², including 32.3 km² of open water (Fig. 1a). The lake is primarily fed by surface runoff and atmospheric precipitation, which accounts for 77% of the total (Liu et al., 2006). The surficial geology is dominated by Triassic limestone; the soils on the slopes of the Lake Yilong catchment are

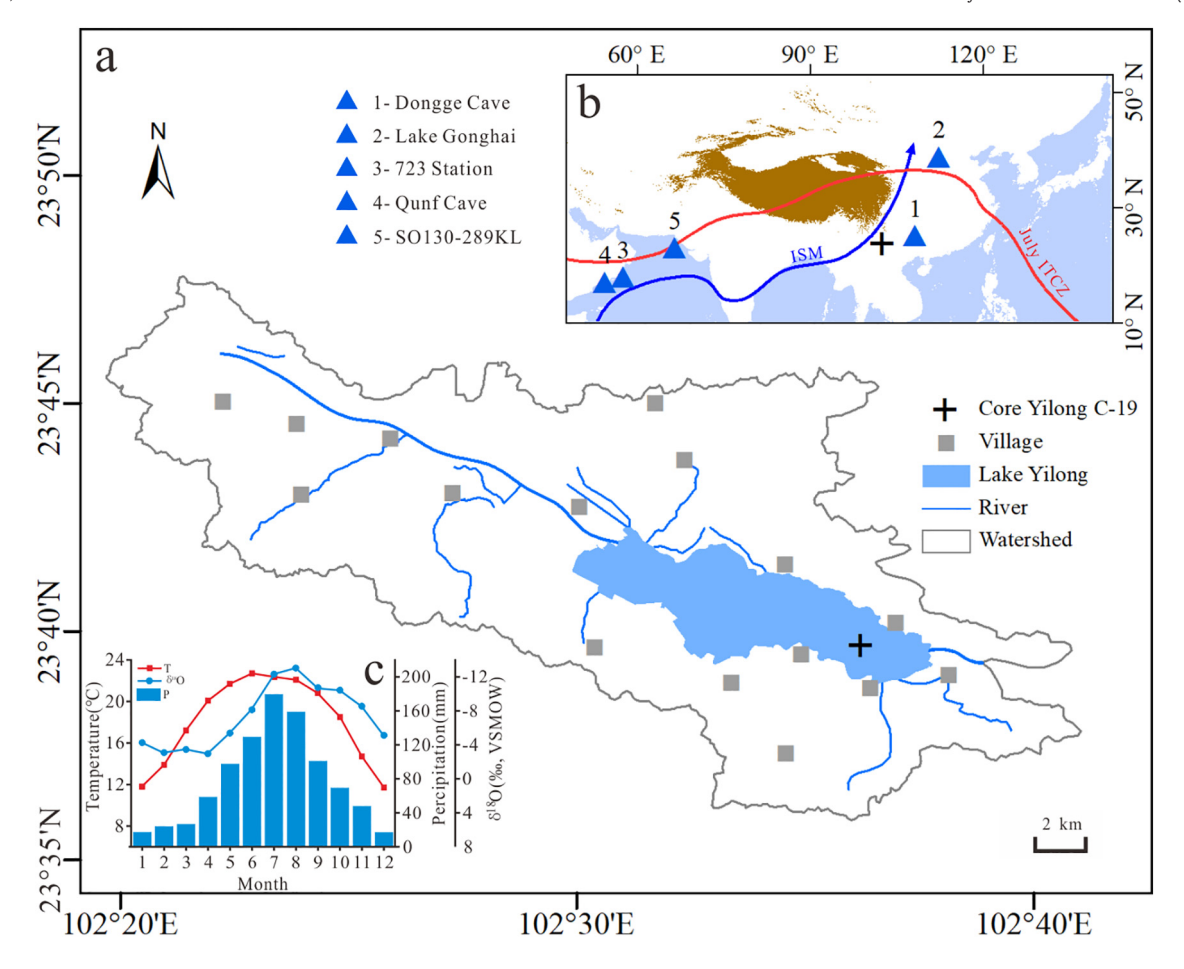


Fig. 1. Information on the modern hydrology and climate in the Lake Yilong watershed. (a) Lake Yilong and its drainage systems. (b) Insert map showing the locations of Lake Yilong (black cross) and cited records from areas dominated by the East Asian Summer Monsoon and the Indian Summer Monsoon (ISM). 1–Dongge Cave (Wang et al., 2005b); 2–Lake Gonghai (Chen et al., 2015); 3–723 station (Gupta et al., 2003), 4–Qunf Cave (Fleitmann et al., 2003), 5–S0130-289KL (Deplazes et al., 2013). The blue arrow indicates the wind direction in the ISM-domains, and the red dotted line depicts the modern location of the ITCZ in July (modified from Wang et al., 2017). (c) The mean monthly precipitation and temperature during 1981–2010 monitored by the Shiping meteorological station in the lake watershed (cited from the Chinese Meteorological Administration), and monthly average oxygen isotope values for 1986–2003 at the GNIP station in Kunming (IAEA/WMO). (For interpretation of the references to colour in this figure legend, the reader is referred to the web version of this article.)

mainly terra rossa (red soil), and the land use around the lake margins is dominated by rice cultivation. The average vegetation coverage in the watershed is ~24% (Zhai et al., 2006).

Most of the precipitation in the region originates in the Bay of Bengal and the Arabian Sea and is supplied via enhanced ISM flow (Fig. 1b; An et al., 2011; Wang et al., 2017); thus the region has the typical characteristics of a monsoon climate in Asia, with wet and warm summers and dry and cold winters. The mean annual temperature during 1981–2010 was 18.1 °C (Fig. 1c), and the mean annual precipitation during the same interval was 923 mm, with ~80% falling in the warmer months from May to October, based on data from instrumental measurements at Shiping meteorological station (Fig. 1c). The annual weighted oxygen isotope composition (δ^{18} O) of modern precipitation at Kunming is -7.3% VSMOW, with negative values in summer and positive values in winter (Fig. 1c).

Previous studies of climatic and environmental changes, including pollution impacts, have been conducted at Lake Yilong (Bai et al., 2011; Li et al., 2018a). A large area of wetland on the lake shore has been converted to cultivated land during the past five decades, which has led to heavy metal contamination of the drainage into the lake due to agricultural activity (Bai et al., 2010). The region surrounding Lake Yilong has experienced intensive human disturbance during the past and there are a large number of archaeological sites dated to the Neolithic through to the historical period (Hu, 1999).

2.2. Sampling and dating

In May 2019 a sediment core (Yilong C-19) was obtained from the center (23°39′N, 102°36′E) of Lake Yilong, in a water depth of 4.3 m, using a steel-barreled Livingston square-rod piston corer. A 31-cm-long gravity core that preserved the interface of water and sediment was also obtained from the same site using a UWITEC gravity corer. Overlapping core sections were correlated based on variations in sediment geochemistry (XRF-Ca), producing a 338 cm–long composite record (Fig. S1). The core sections were collected in half-section polyethylene tubes and kept at 4 °C prior to analysis. The core sections were split lengthwise, photographed, and the lithology described in the laboratory. They were then cut into contiguous 0.5-cm slices for various laboratory analyses.

Thirteen samples, including charcoal and terrestrial and aquatic plant macrofossils, were picked for accelerator mass spectrometry (AMS) ¹⁴C dating which was conducted by Beta Analytic (Florida, USA); standard pretreatment procedures were used, with acid, base and acid, in sequence (Olsson, 1986). The AMS ¹⁴C dating results were calibrated to calendar years before the present (BP, before 1950 CE) using CALIB 8.0.1. The chronology of the sediment core was then established with smoothing spline functions using the Clam library (Blaauw, 2010) with the updated IntCal20 calibration curve (Reimer et al., 2020), implemented with the "R" package. As the age control points are insufficient to capture the age of the base of the core, only

the age model for the section above 314.5 cm was successfully established.

2.3. Geochemistry measurements

The archive half of the core was flattened and covered by 4 µm—thick Ultralene film, and then nondestructive continuous X-ray fluorescence (XRF) core scanning was performed at a 2-mm resolution to determine relative element concentrations, using an Avaatech XRF core scanner (Weltje and Tjallingii, 2008). Al, Si, S, Cl, K, Ca, Ti, Mn and Fe were detected at 1 mA and 10 kV for 15 s; and Cu, Zn, Ga, Br, Rb, Sr, Y, Zr, Nb and Pb were detected at 2 mA and 30 kV for 25 s. Given that the XRF results are potentially influenced by water content, surface roughness, and grain-size variations (Weltje and Tjallingii, 2008), and the natural abundance of each element is different, it is necessary to normalize the raw counts. As the five conservative elements Al, Si, K, Rb, Ti are significantly positively correlated (Fig. S2), they were selected and normalized. The intensities of the selected elements were normalized individually using the formula:

$$N_i = (X_i - X_{min})/(X_{max} - X_{min}) \tag{1}$$

where N_i is the normalized value of corresponding element i; X_i is the measured counts; and X_{min} and X_{max} represent the minimum and maximum of X_i , respectively. The normalization yields values between 0 and 1. The normalized values from the five selected elements were further averaged and the result is denoted I, which is regarded as an index of the relative content of clastic material from the terrestrial catchment.

The magnetic susceptibility (MS) was measured using a Bartington Instruments MS2 meter attached to the XRF scanner. Contents of organic matter (OM) and carbonate were assessed by measurements of loss-on-ignition (LOI) at 550 °C and 950 °C, respectively, based on the assumption that the combustion of OM at 550 °C is sufficient and the loss of mass at 950 °C was caused by the decomposition of carbonate to oxide and CO₂. The CO₂-induced mass loss was multiplied by the ratio of the molecular weights of CaCO₃ and CO₂ (2.27) (Dean, 1974). Contents of total organic carbon (TOC) and total nitrogen (TN) were measured on 250 samples which were pretreated with HCl to remove inorganic carbon, and carbon/nitrogen (C/N) ratios were then calculated based on the results (Meyers, 1997). The sediment core was subsampled at 0.5–2.0-cm intervals for measurements of carbonate stable oxygen isotopes ($\delta^{18}O_{carb}$) and stable carbon isotopes ($\delta^{13}C_{carb}$). After treatment with 10% H₂O₂ to remove OM, the sub-samples were passed through a 62-µm mesh screen in order to remove biological carbonates including gastropod shells and ostracods (Nelson et al., 2011). Samples were measured using a MAT 252 gas-ratio mass spectrometer coupled with a KIEL-III carbonate preparation device at the Environmental Isotope Laboratory, University of Arizona. In order to identify the mineral phase, 17 samples were lyophilized, homogenized and then analyzed for powder X-ray diffraction (XRD) using an X'Pert Pro MPD Powder X-ray Diffractometer operating at 40 kV and 40 mA with Cu K α radiation, at the Key Laboratory of Western China's Environmental Systems. In addition, selected samples were analyzed on a Thermo Fisher Apreo S Scanning Electron Microscope (SEM) to identify the morphology and crystal structure based on standard procedures (Xie, 1984).

3. Results

3.1. Chronology and geochemical stratigraphy

The AMS ¹⁴C dating results are listed in Table 1. AMS ¹⁴C dates from terrestrial plant macrofossils (including charred material) were used to construct an initial age-depth model, assuming that they are relatively close to the depositional age of the sediments. However, dating results from aquatic plant material may be influenced by the carbon reservoir effect which is caused by ¹⁴C depletion in the lake water (MacDonald et al., 1987), and its possible influence should be assessed or even corrected. The carbon isotope ratios of the dated aquatic plant materials are relatively negative, varying from -23.4% to -15.7% (Table 1), which are similar to the values of terrestrial C₃ plants (Chappuis et al., 2017). Although the δ^{13} C values of freshwater aquatic plant material is not as clear an indicator of the photosynthetic pathway as in terrestrial plants (Keeley and Sandquist, 1992), the relatively negative δ^{13} C values from Lake Yilong indicate that the dating materials may be derived from emergent macrophytes or phytoplankton. Lake Yilong is an open shallow lake supplemented by precipitation, and therefore the rate of CO₂ exchange between the lake water and the atmosphere is relatively high, leading to a limited carbon reservoir in the lake. In addition, all of the dates are in stratigraphic order and the intercept of the final age model (the age of the core top) is nearly zero. Therefore, it is concluded that the aquatic plants used for dating largely avoid the carbon reservoir effect which usually occurs in the lakes in Yunnan (Zhou et al., 2015; Li et al., 2018a). The final age-depth model is shown in Fig. 2b.

In terms of lithology (Fig. 2a) the core can be divided into the following intervals. (i) 338–299 cm (before 9700 cal yr BP): homogenous black clay-silt with no visible sedimentary structures, composed of ~80% clastic material and ~12% organic matter (Fig. 2e–f), with an extremely low sediment accumulation rate (0.005 cm/yr) (Fig. 2c). (ii) 299–290.5 cm (9700–8700 cal yr BP): reddish sediments with higher MS values (Fig. 2d). (iii) 290.5–38.1 cm (8700–1450 cal yr BP): clastic material, the proportion of which decreases upwards, while the carbonate content increases (Fig. 2g), and the organic matter content fluctuates. The top consists of a thick layer of greyish carbonate mud with a carbonate content up to ~90%. The mean rate of sediment

Table 1Accelerator mass spectrometry (AMS) ¹⁴C and isotope ratio mass spectrometry (IRMS) ¹³C dates for sediment core C-19 from Lake Yilong.

Beta No.	Sample name	Composite depth (cm)	Sample material	IRMS δ ¹³ C (‰)	¹⁴ C age (yr BP)	Error (yr)	Calibrated age (cal yr BP, 2σ)	Median age (cal yr BP)
535118	Yilong C-19(D1) 16-17 cm	24.5	Aquatic plants	_	890	30	728-906	783
535120	Yilong C-19(D1) 62.5-63 cm	71	Charred material	-15.1	2610	30	2719-2769	2745
535121	Yilong C-19(D1) 80-81 cm	88.5	Terrestrial plants	-29.4	2820	30	2848-3055	2921
535123	Yilong C-19(D2) 13-14 cm	118.5	Aquatic plants	-15.7	3520	30	3698-3879	3782
535124	Yilong C-19(D2) 30-31 cm	135.5	Aquatic plants	-17.1	4250	30	4653-4864	4836
535125	Yilong C-19(D2) 63-64 cm	168.5	Aquatic plants	-18	4820	30	5477-5596	5522
535126	Yilong C-19(D3) 25-26 cm	193.5	Aquatic plants	-18.4	5000	30	5604-5891	5723
535127	Yilong C-19(D3) 40-41 cm	208.5	Aquatic plants	-20.1	5700	30	6401-6600	6478
535128	Yilong C-19(D3) 60-61 cm	228.5	Aquatic plants	-20.5	6240	30	7016-7254	7168
535130	Yilong C-19(D3) 90-91 cm	258.5	Aquatic plants	-23.4	6360	30	7169-7416	7284
535131	Yilong C-19(D4) 38-39 cm	277.5	Aquatic plants	-19.1	6990	30	7728-7930	7824
535132	Yilong C-19(D4) 53-54 cm	292.5	Terrestrial plants	-29	7860	30	8549-8771	8634
535133	Yilong C-19(D4) 75-76 cm	314.5	Terrestrial plants	-25.4	10,470	40	12,105-12,620	12,493

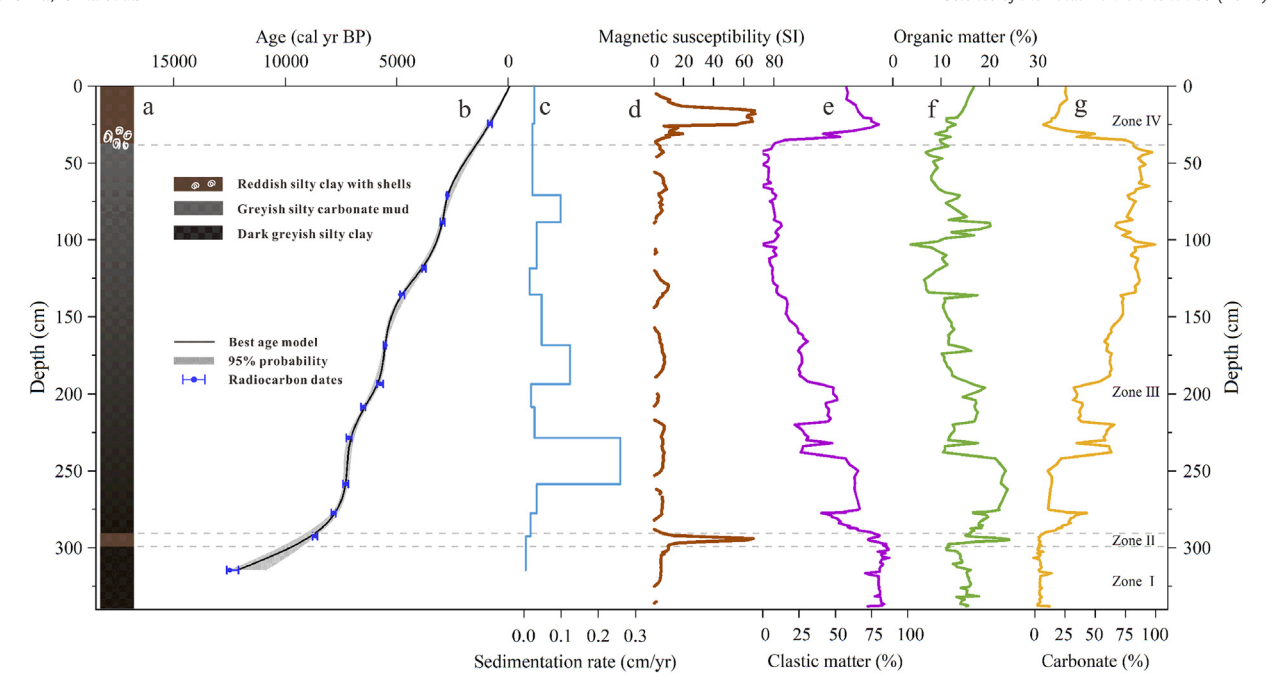


Fig. 2. Chronostratigraphy and lithological composition of core C-19 from Lake Yilong. (a) Stratigraphic column; (b) age-depth model; (c) sediment accumulation rate; (d) magnetic susceptibility; (e) clastic material content; (f) organic matter content; (g) carbonate content.

accumulation is 0.035 cm/yr (Fig. 2c). (iv) 38.1–0 cm (the last ~1450 years): the carbonate content decreases abruptly and the sediments are composed of fine-grained, reddish silt-clay with a conspicuous shell layer at the base (Fig. 2a, g). The MS values increase rapidly at the same time and reach a peak at 16 cm (~500 cal yr BP) and then decrease sharply, accompanied by an increase in clastic material (Fig. 2d–e).

3.2. Geochemical proxies

Based on the trends of the element counts and concentrations of TOC and TN, together with those of the C/N and isotopic ratios, the records can be divided into the following four zones (Figs. 2–3).

Zone I (338–299 cm, before 9700 cal yr BP) is characterized by relatively uniform values of the proxies. Index I and the clastic material content are at their highest levels, while the contents of TOC and TN are low, with average values of ~5.5% and ~3.3%, respectively (Fig. 3); however, the C/N ratio reaches its highest value. The values of $\delta^{18}O_{carb}$ and $\delta^{13}C_{carb}$ are at minimum levels, with values averaging -19.6% VPDB and -1.24% VPDB, respectively.

Zone II (299–290.5 cm, 9700–8700 cal yr BP) corresponds to a pronounced change in sediment composition. Index I and the Fe/Mn ratio fluctuate and reach minimum values, while Ca increases slightly forming a minor peak. The contents of TOC and TN increase from the middle of the zone while the C/N ratio decreases, and $\delta^{18}O_{\text{carb}}$ and $\delta^{13}C_{\text{carb}}$ increase sharply at the beginning of the zone and then remain consistently high, but with an abrupt decrease at the end of the zone. The MS is high throughout.

Zone III (290.5–38.1 cm, 8700–1450 cal yr BP) is characterized by a high carbonate content. Index I exhibits an overall decreasing trend which tracks the clastic content. TOC and TN increase significantly with distinct peaks during 7700–7200 cal yr BP, and then decrease overall but with very large fluctuations. $\delta^{18} O_{carb}$ and $\delta^{13} C_{carb}$ show a similar increasing trend.

Zone IV (the uppermost 38.1 cm, 1450 cal yr BP to the present) contrasts sharply with the other three zones because of its reddish sediments, high MS values, and the high content of clastic material

indicated by high values of index I. The contents of TOC and TN decrease until ~600 cal yr BP and then increase, which is similar to the variations of Ca intensity. $\delta^{18}O_{carb}$ continues an increasing trend, although the resolution is low, but $\delta^{13}C_{carb}$ decreases.

4. Discussion

4.1. Environmental significance of lacustrine carbonate $\delta^{18}O$ and other sedimentary parameters

Carbonates are common minerals in lake sediments and are mainly composed of terrigenous, endogenetic and authigenic forms (Moreno et al., 2011). Only the δ^{18} O of endogenetic carbonate can be regarded as a useful palaeoclimatic proxy in lake sediments because it originates from chemical processes in the water column. In addition, given that different minerals have different levels of mineral-water fractionation (Leng and Marshall, 2004), the determination of the carbonate mineral phase is worthy of attention.

The carbonate content of the sediments of Lake Yilong during ~12,000-9700 yr BP is quite low (Fig. 2g), and the XRD analysis results indicate that there is no clear carbonate mineral phase. Carbonate is widely distributed in southwestern China, and the variations in Ca values, which represent the sedimentary carbonate content, are consistent with the changes in index I, which represents clastic input from the catchment (Fig. S3). Therefore, the sedimentary carbonate content during this period is of detrital origin. Siderite is the primary carbonate mineral identified by XRD analysis in the sediments during the subsequent Zone II (Fig. S4). Because the variation in the Fe content contrasts with that of index I during this interval, and siderite is mainly formed by lake endogenetic precipitation, its isotopic composition is a valuable indicator of the sedimentary environment (Mozley and Wersin, 1992). The extremely positive δ^{13} C of the authigenic carbonate suggests an aquatic environment with a CO₂-source strongly enriched in ¹³C, and the high $\delta^{18}O_{carb}$ values indicate the enrichment of ^{18}O due to evaporation (Bahrig, 1989).

The results of XRD analysis of samples from sediment deposited during *Zones* III and IV indicate that calcite is the primary carbonate

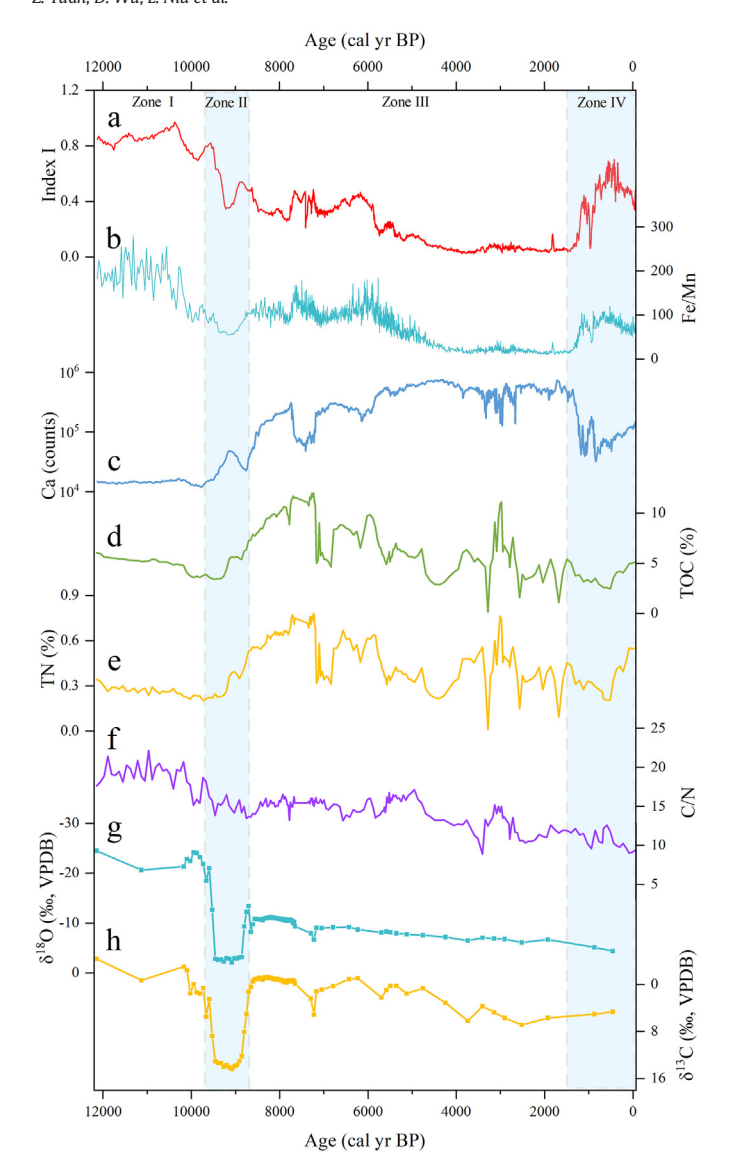


Fig. 3. Time series of various sedimentary parameters from core C-19. Index I (composed of Al, Si, K, Ti, Rb) (a), Fe/Mn ratio (b), Ca counts (c), TOC content (d), TN content (e), C/N ratio (f), carbonate δ^{18} O (g), and carbonate δ^{13} C (h). The interval of 9.7–8.7 kyr BP and the period during the last ± 1500 years are shaded.

mineral (Fig. S4); moreover, SEM images show that the calcite crystals have a euhedral or slightly subhedral morphology (Fig. S5), indicating precipitation from the water column. The concentrations of carbonate and organic matter are positively correlated during some intervals, suggesting that carbonate precipitation and primary productivity at Lake Yilong were inter-related. The C/N ratio is widely used to distinguish the sources of sedimentary organic matter (Meyers, 1997). The overall decreasing trend of the C/N ratios indicates the increasing contribution of authigenic OM to the sediments, demonstrating the role of aquatic plants consuming CO₂ and promoting the precipitation of endogenetic carbonate. In addition, the significant negative correlations between Ca and index I in Zones III and IV (the Pearson correlation coefficients are -0.79 and -0.77, respectively) suggest that carbonate was no longer supplied to the lake as a component of the clastic sediments (Fig. S3). This demonstrates that the carbonates in the Lake Yilong sediments during the most recent two periods are authigenic calcites, the δ^{18} O and δ^{13} C values of which can be used to reconstruct variations in climate and hydrology.

 $\delta^{18}O_{carb}$ is controlled by the oxygen isotopic composition of the lake water and the temperature when it precipitates (Craig, 1965; Leng and Marshall, 2004). The equilibrium isotopic fractionation between water and carbonate controlled by temperature is around -0.24%/°C (Craig. 1965), and the very large range of variation of $\delta^{18}O_{carb}$ in the sediments of Lake Yilong during the 9.3 ka event and in the middle to late Holocene (~18‰, ~6‰, respectively) was not controlled principally by temperature. Thus, the fluctuations of $\delta^{18}O_{carb}$ were dominated by the variation of the δ^{18} O of the lake water, which has been suggested to be controlled by the oxygen isotopic composition of precipitation and temperatureinduced evaporation from the lake surface (Leng and Marshall, 2004). Lake Yilong is mainly fed by rivers and it behaves as an open-basin lake. In such lakes with a limited watershed area and short water residence time, $\delta^{18}O_{carb}$ is mainly controlled by the mean annual precipitation (Mckenzie and Hollander, 1993). Because the total amount of the precipitation in monsoonal regions is mainly contributed by the rainfall during the summer, $\delta^{18}O_{carb}$ is largely controlled by the summer precipitation. Thus, the long-term variability of $\delta^{18}O_{carb}$ in the sediments of Lake Yilong should represent the changing intensity of precipitation in the ISM domains, which is also the case for δ^{18} O records from lacustrine sediments and cave deposits in southwestern China (e.g., Wang et al., 2005b; Wu et al., 2018; Hillman et al., 2020).

4.2. Natural and human impacts on the Yilong lake watershed ecosystem since ~12,000 cal yr BP

4.2.1. Relatively stable hydrological conditions from the late Pleistocene to the beginning of the Holocene

The element contents of lake sediments not only reflect the sedimentary provenance but they can also be used to indicate geochemical responses to environmental change (Goldberg et al., 2000; Tanaka et al., 2007). Index I is the averaged contents of Al, Si, K, Ti, and Rb, which are inert elements and are mainly preserved in weathering products such as clastic materials (e.g., quartz, mica) or non-residual materials (e.g., clay, iron oxides) (Li et al., 2015). According to the results of XRD analysis, the dominant mineral in the late Pleistocene interval of the core is quartz, which is a terrigenous clastic component generated by physical erosion and directly transported to the lake via fluvial inputs and/or as surface runoff (Fig. S4; Shen, 2009). Although index I and the content of detrital materials vary synchronously, with high values, during this period, considering the low sediment accumulation rate, physical erosion within the watershed was limited. The low values of carbonate content and Ca counts indicate that the water level of the lake was high as calcium ion is not readily precipitated when it is diluted (Chen et al., 2015). Therefore, a possible explanation for the variations of the counts of Fe and Mn is that Mn is dissolved faster in a deep-water anoxic environment, while much undissolved Fe was stored in sediments during this interval (Davison, 1993). In summary, there was a stable lake with a high lake level during the late Pleistocene and early Holocene.

The low sedimentary organic matter content, combined with low MS values and a high influx of primary minerals, indicates that soil development was weak during this interval, as terrestrial vegetation growth was limited by the cold climate (Wu et al., 2018). TOC and TN are linearly related ($R^2 = 0.87$) and the value of the intercept is low (Fig. S6), suggesting that nitrogen is mainly present in organic form, and thus the C/N ratio directly reflects the origin of the OM (Liu et al., 2010; Zhang et al., 2015). The high C/N ratios during this interval indicate that the OM in the sediments was mainly derived from terrestrial sources (Meyers, 1994). It has been found that seasonal variations in temperature and rainfall are positively correlated in the monsoonal region of Asia, and the TOC content of lacustrine sediments in the region can indicate precipitation amount (An et al., 2011). Therefore, based on the low content of OM in the sediments during this period, it can be inferred that the environment in the early Holocene did not ameliorate significantly and remained as cold and humid as in the late Pleistocene.

Most of the proxies from Lake Yilong during this period show low-amplitude fluctuations indicating the absence or non-recording of sub-orbital (millennial-scale) events that are documented during the transition from glacial interglacial condition elsewhere. During the last deglaciation, there were a series of abrupt climatic events: the cold Heinrich 1 (H1), the warm Bølling-Allerød (BA) and the cold Younger Dryas (YD) (Heinrich, 1988; Shakun and Carlson, 2010; Denton et al., 2010), which are documented in several lacustrine records from the Yunnan Plateau (Chen et al., 2014b; Li et al., 2018b; Zhang et al., 2019). However, it appears that there may be regional differences in the impacts of these events (Singer et al., 1998), and their geographical distribution and timing are still under discussion (Cheng et al., 2020b).

4.2.2. The 9.3 ka dry climatic event (9700–8700 cal yr BP)

The paleoclimatic reconstruction reveals a centennial-scale regional climatic event during the interval from 9700 to 8700 cal yr BP; it is highlighted by more positive $\delta^{18} \text{O}_{\text{carb}}$ values with sharply increased and decreased values at the beginning and end, respectively (Fig. 4a, b). Index I decreases during this interval, indicating a weakening of physical erosion in the watershed and a decrease in runoff. The enrichment of Mn in the sediments may have been caused by the preferential removal of Mn in the poorly ventilated lake mud around the lake margin which was exposed to the surface under the arid climate; therefore, the mobilized Fe and Mn were stored in the sediments after entering the shallow lake which had an oxidizing environment (Fig. 4c-e; Mackereth, 1966). Combined with the isotopic records, it can be concluded that an intense drought event occurred in the region, which resulted in a shallower lake and the deposition of silty sediments. In addition, the increased accumulation of Fe and the formation of siderite may have contributed to the high MS values.

The early Holocene millennial-scale rapid climatic evident in the reconstruction can be compared with other records from the ISM domain. A record of Globigerina bulloides from rapidly accumulating and minimally bioturbated sediments in the continental margin of Oman indicates that a centennial-scale weak monsoon event occurred at ~9400 yr BP (Fig. 4h; Gupta et al., 2003), which is consistent with the reflectance record of sediments from the Arabian Sea (Fig. 4g; Deplazes et al., 2013). In addition, values of stalagmite δ^{18} O from Dongge cave in Guizhou Province in southwestern China show a slight decrease at the beginning of the Holocene, followed by an abrupt increase at ~9300 cal yr BP, suggesting a significant decline of the ISM (Wang et al., 2005b). A similar pattern occurs in δ^{18} O records of stalagmite from Qunf cave in Oman, southeastern Arabian Peninsula (Fleitmann et al., 2003). In addition, a pollen-based precipitation record from Lake Gonghai in the EASM domains demonstrates that insolation-driven EASM variability was punctuated by millennial-scale EASM weakening during the interval of ~9500-8500 yr BP (Chen et al., 2015). Although these records are from different geological archives and there are a minor differences in the timing of their initiation, they all document a decrease in monsoon precipitation at 9.3 ka.

Millennial-scale precipitation variability in different monsoon regions shows a high degree of temporal consistency and it is also correlative with rapid climatic events reconstructed from the North Atlantic region (Broecker et al., 1992; Clement and Peterson, 2008). Based on the ice-rafted detritus content of sediment cores, Bond et al. (1997) first studied cold events in the North Atlantic; nine cold events were identified during the Holocene (Fig. 4f; Bond et al., 2001), which were closely linked with decreases in Atlantic Meridional Overturning Circulation. Among them, the ~9.2 ka cold event resulted from a meltwater pulse, although it was weaker than the 8.2 ka event which was recorded globally. Yu et al. (2010) attributed the widespread climate anomaly some 9300 years ago to the destruction of a glacial drift dam in the southeastern corner of Lake Superior, which caused the influx of a large volume of freshwater to the North Atlantic, thus accelerating the melting of the Arctic or Greenland ice sheets (Rasmussen et al.,

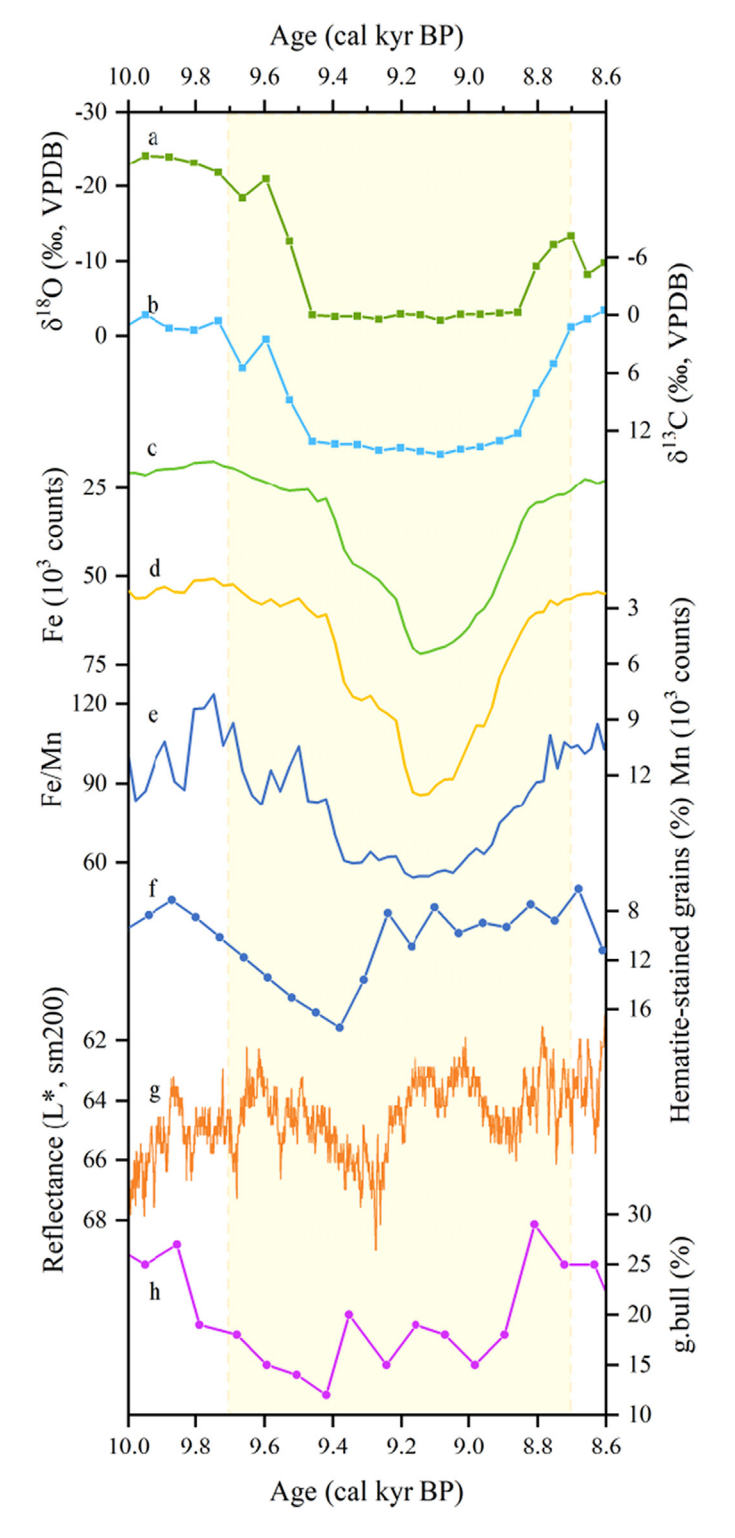


Fig. 4. The drying event during 9.7–8.7 ka and its possible forcing factors. (a) δ^{18} O record from Lake Yilong; (b) δ^{13} C record from Lake Yilong; (c) Fe content; (d) Mn content; (e) Fe/Mn ratio; (f) stacked record of North Atlantic drift ice indices (Bond et al., 2001); (g) total reflectance (L*) of sediments from the Arabian Sea (Deplazes et al., 2013); (h) percentages of *G. bulloides* in ODP Hole 723A in the Arabian Sea (Gupta et al., 2003).

2007). Geological observations and numerical simulation show that the injection of freshwater into the North Atlantic may cause significant changes in deep water and meridional circulation in the North Atlantic, resulting in the southward movement of the ITCZ (Broccoli et al., 2006; Menviel et al., 2008). Due to the annual

variation of solar insolation, the ITCZ moves seasonally, resulting in a pressure gradient across the equator and the formation of the tropical monsoon (Tomas and Webster, 1997). As a subsystem of the tropical monsoon, the intensity of the ISM will decrease with this southward movement of the ITCZ (Chiang and Bitz, 2005; Deplazes et al., 2013).

4.2.3. Persistent drying in the ISM domains during the middle to late Holocene

At Lake Yilong, both the TOC content and the C/N ratio varied synchronously during the last ~8700 years, with an overall decreasing trend (Fig. 3d, f). This indicates that the contribution of the OM from terrestrial sources to the lake sediment decreased during the middle to late Holocene, corresponding to a further decline of the ISM. The record of the oxygen isotopes of carbonate and other indexes from Lake Yilong during the last 8700 years therefore indicates that the regional climate was wet from 8500 to 6500 cal yr BP (Fig. 5a), resulting in a maximum of organic productivity in the region. All of the proxies suggest that the ISM experienced a gradual weakening since the early Holocene, with the weakest monsoon occurring during the late Holocene, consistent with the variation of July insolation at low latitudes in the Northern Hemisphere (23°N) (Fig. 5g).

Previous studies have indicated that the δ^{18} O of authigenic lacustrine carbonate can be used to track the variation of monsoon precipitation over the Asian continent (Wei and Gasse, 1999). Yunnan is situated in the region of ISM influence and several records of carbonate $\delta^{18}\mbox{O}$ from lakes on the Yunnan Plateau have been obtained. Lake Qilu and Lake Xingyun are located to the north of Lake Yilong and the carbonate δ^{18} O records from their sediments indicate a consistent trend with gradually increasing values since ~9000 yr BP (Fig. 5b-c; Hillman et al., 2017, 2020; Wu et al., 2018). Overall, the various carbonate δ^{18} O records from lake sediments from Yunnan demonstrate that the strength of the ISM decreased during the middle to late Holocene. Stable isotope records from stalagmites are widely used to reflect variations of the Asian summer monsoon, although their precise environmental significance for eastern Asia is still debated (Maher, 2008; Tan, 2014; Liu et al., 2020). The stalagmite δ^{18} O records from Hoti cave and Qunf cave in Oman show a decrease after 6300 yr BP and after 7800 yr BP, indicating decreases in precipitation (Fig. 5e; Neff et al., 2001; Fleitmann et al., 2003). Moreover, the record of speleothem δ^{18} O from Dongge cave in China shows a similar pattern of variation with the ISM (Fig. 5d; Wang et al., 2005b). All of the isotopic records mentioned above show the same trend of variation as the precipitation reconstruction based on pollen assemblages from Lake Xingyun (Fig. 5f; Chen et al., 2014a).

These varied marine and terrestrial records point to a southward movement of the ITCZ during the middle to late Holocene and hence a gradual decline in the intensity of the ISM. The same decrease of the ISM observed at Lake Yilong and in other archives supports the conclusion that the evolution of the ISM on the orbital timescale is forced predominantly by Northern Hemisphere summer insolation (Kutzbach and Guetter, 1986; Prell and Kutzbach, 1992). However, a recent 15,000-yr lake level reconstruction from Lake Chenghai in Yunnan Province, interpreted primarily as a precipitation record, indicates that lake levels, hence precipitation, were high during the BA interstadial and the early and late Holocene, but were low during the middle Holocene (Xu et al., 2020). This pattern is out-of-phase with summer insolation in the Northern Hemisphere on the orbital timescale. However, it should be noted that Xu et al. (2020) did not consider issues such as the fact that radiocarbon dates from gastropod shells preserved within lake sediments may be influenced by the carbon reservoir effect, and that Yunnan has experienced intensive human activities, including land clearance, cultivation and lake water management, which have substantially altered the landscape and the water

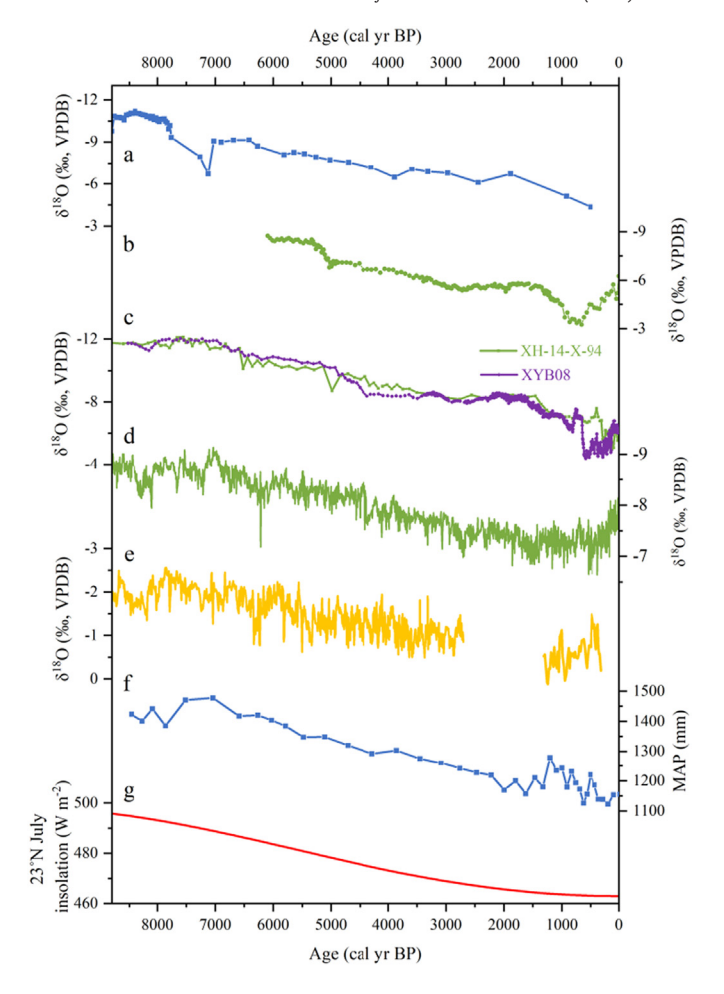


Fig. 5. Comparison of various regional paleoclimatic records. Carbonate δ^{18} O records from Lake Yilong (a) (this study), Lake Qilu (b) (Hillman et al., 2020) and Lake Xingyun (c) (Hillman et al., 2017; Wu et al., 2018); speleothem records from Qunf Cave (d) (Fleitmann et al., 2003) and Dongge Cave (Wang et al., 2005b); reconstructed mean annual precipitation based on pollen assemblages from Lake Xingyun (f) (Chen et al., 2014a), and July insolation at 23°N (g) (Laskar et al., 2004).

resources of the region, at least during the last 1500 years (Dearing et al., 2008; Wu et al., 2015a; Hillman et al., 2016).

4.2.4. Variation of the intensity of regional human activity during the past \sim 1500 yr

The isotopic and elemental records from Lake Yilong reveal a pronounced change after 1450 cal yr BP, highlighted by an obvious increase in the input of terrestrial material against the background of a drying climate. Agriculture and related human activities have significantly altered the landscape of Yunnan during the late Holocene, and therefore it is possible that the regional environmental instability revealed by the large fluctuations of the proxy records since ~1500 yr BP was a function of both climatic changes and human activities. Variations in the strength of the ISM are recorded by the carbonate $\delta^{18}\text{O}$ record from Lake Xingyun, ~80 km northeast of Lake Yilong, which suggest that the strength of the ISM was weak during the past 2000 years, with several abrupt changes (Wu et al., 2018). However, a comparison with independent climatic reconstructions reveals that climate change was not responsible for the abrupt changes in sedimentary indexes at Lake Yilong. The rapid increase in index I since ~1500 cal yr BP indicates the increased input of clastic minerals such as quartz, which is confirmed by the XRD results. It is likely that clearance for agricultural development resulted in the exposure of the surface soil, causing intensified soil erosion. In addition, the high sedimentary MS values

reflect the increasing input of iron-rich soils from the watershed due to the destruction of the natural vegetation by humans (Fig. 2d). Notably, a decrease in C/N ratios after ~600 yr BP suggests a weakening of soil erosion and a rise in the productivity of the lake water, which may have been induced by the increased accumulation of authigenic organic matter caused by cultural eutrophication.

Although the regional environment of Yunnan had been significantly influenced by human activities during the late Holocene, their exact timing is controversial. High-resolution records of charcoal and pollen from Lake Chenghai indicate that after 1860 cal yr BP the climate gradually became drier gradually and there was an increase in the intensity of human activity, including slash-and-burn agriculture and deforestation (Xiao et al., 2018). The onset of early human impacts at ~7000 yr BP has been suggested (e.g. Shen et al., 2005; Dearing et al., 2008), with additional impacts during the last 1000 years (Wu et al., 2015b; Hillman et al., 2016, 2018), or since ~5000 yr BP (e.g. Wang et al., 2016; Sun et al., 2018). Although these conclusions may be influenced by chronological errors and regional differences in human

activities, all of the records demonstrate the significant influence of human activities on the natural environment of Yunnan during the late Holocene.

4.3. Differences in lake ecosystem responses to millennial-scale climatic events and human impacts

With the abrupt drying of the climate during the 9.3 ka event, runoff in the Lake Yilong watershed decreased gradually, resulting in the steady weakening of soil erosion (Fig. 6a–b). However, the variations of TOC and TN exhibit a slight lag compared with the abrupt hydrological shift during this event (Fig. 6e-f), suggesting a lagged biological response to environmental changes (Jones et al., 2012). The notable shifts in C/N ratios indicate a phase of increased productivity in the lake and the enhanced recycling of aquatic OM between the sediments and the water column, which further indicates that the structure and functioning of the lake ecosystem have changed (Fig. 6d–e; Wolfe et al., 1999). Significantly, the lake ecosystem gradually recovered at the end of the

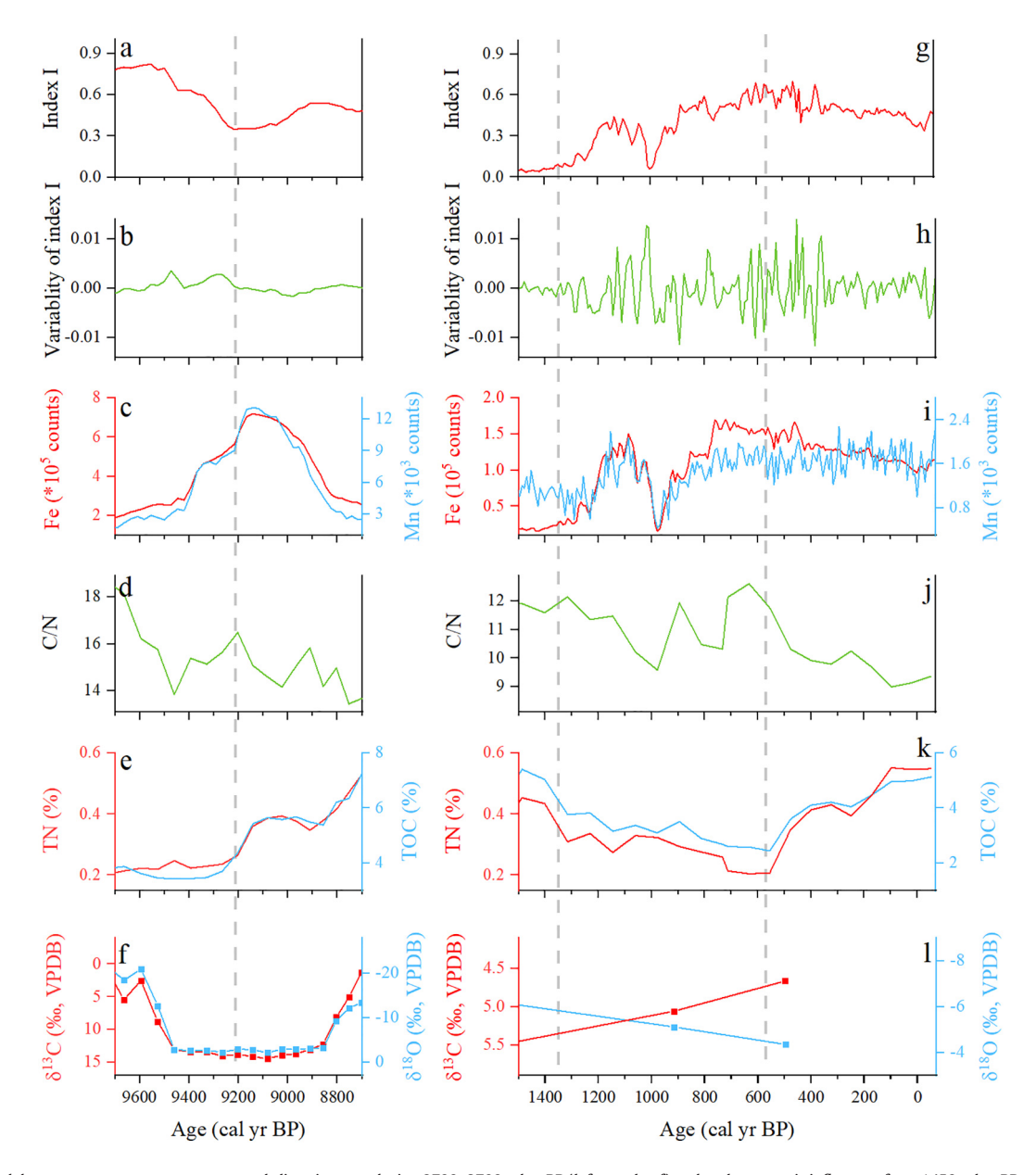


Fig. 6. Contrasting lake ecosystem responses to a natural climatic event during 9700–8700 cal yr BP (left panel, a-f) and anthropogenic influences from 1450 cal yr BP to the present (right panel, g-l). (a, g) index I; (b, h) index I; (c, i) Fe and Mn counts; (d, j) C/N ratio; (e, k) TOC and TN contents; (f, l) carbonate δ^{18} O and δ^{13} C.

9.3 ka event, which is indicated by the fact that the runoff, water level and area of the lake, soil erosion, and primary productivity all increased and subsequently remained relatively stable.

During the last millennium, human activities significantly influenced the ecosystem in the Lake Yilong watershed. The intensity of the soil erosion increased substantially, accompanied by very high variability, as a consequence of deforestation, agriculture and mining (Fig. 6g-i). A decrease in organic productivity in the watershed preceded the increase in the intensity of soil erosion, which may also have been closely related to human activity. After ~600 yr BP, the contents of sedimentary TOC and TN increased and the C/N ratio decreased, suggesting an increasing supply of authigenic organic matter to the sediments, and hence enhanced lake primary productivity, which was a response to an increased nutrient supply (Fig. 6j-k). In addition, large numbers of spiral gastropod shells, possibly Margarya mansuyi (Liu et al., 1979), are present at the base of Zone IV, corresponding to a lithological change; however, the subsequent disappearance of Margarya mansuyi may have been the result of human disturbance of the lake system (Shen et al., 2005).

A comparison of the responses of Lake Yilong to the 9.3 ka climatic event with that to later human impacts was made to highlight the possible differences. Negative feedback promotes ecosystem stability by enhancing resilience to disturbance, while positive feedback has the opposite effect (Walker and Meyers, 2004). The lagged response of the lake system to natural climatic events indicates strong resilience at times when the structure of the lake ecosystem was relatively simple. However, in response to long-term anthropogenic interventions, the lake ecosystem became fragile and unstable, and positive feedback was strengthened and the lake ecosystem shifted far from its previous relatively stable state.

A threshold is defined as the transition from negative feedback to positive feedback, and a discontinuous transition is initiated by a triggering factor which represents a change in specific biological or abiotic variables (Stringham et al., 2003; Briske et al., 2006). Human activities after ~800 yr BP evidently exceeded an ecological threshold at Lake Yilong which resulted in a major shift of the structure of the ecosystem in the lake watershed, which resulted in a decrease in soil erosion and a rapid increase in lake productivity. The occurrence of this transition implies the possibility that a critical threshold existed at Lake Yilong. It is worth noting that an ecosystem steady-state tends to exist, as indicated by the finding that ecosystems maintain a stable state through the internal balances and self-regulation on a long timescale after an anomalous climatic event. However, the record from Lake Yilong indicates that human activities directly damaged the system structure and which resulted in a rapid response to the forcing.

5. Conclusions

A continuous and well-dated sedimentary record has been obtained from Lake Yilong in Yunnan Province, southwestern China, in order to reconstruct hydro-climatic variations and lake ecosystem responses to climatic and anthropogenic impacts during the past ~12,000 yr. Multiple geochemical proxy records from the sediments indicate that the cold and humid environment during the last deglaciation and early Holocene was interrupted by a drought during 9700-8700 cal yr BP. Precipitation decreased during this event, resulting in a gradual decrease in the level of watershed soil erosion. The structure of the lake system changed slightly and finally recovered from the impact of this environment perturbation because of its relatively high-level of resilience. Thereafter, a trend of persistent drying occurred during the middle and late Holocene, and there was an increase in the intensity of human activity during the past 1500 years. Under the influence of an increasing human population and intensive human activities, the terrestrial landscape and the lake ecosystem underwent significant changes. The intensity of soil erosion increased significantly as a consequence of deforestation and agriculture, and the lake ecosystem changed from an environment with a low productivity to a eutrophic state. Therefore, positive feedback effects were strengthened as a consequence and the lake ecosystem became unstable and entered a state which was quite different compared to its previous relatively resilient state. An important finding of the study is that the impacts of human activities on the lake ecosystem exceeded those a natural climatic event, and that the deterioration of the lake environment and irreversible impacts will continue unless the lake environment is protected.

CRediT authorship contribution statement

D Wu designed research; ZJ Yuan, D Wu, LL Niu, XY Ma and YM Li performed research; ZJ Yuan, D Wu, A Hillman, M Abbott and AF Zhou analyzed data; ZJ Yuan and D Wu wrote the paper; D Wu, A Hillman and M Abbott revised the paper.

Declaration of competing interest

The authors declare that they have no known competing financial interests or personal relationships that could have appeared to influence the work reported in this paper.

Acknowledgments

This research was supported by the National Natural Science Foundation of China (Grant Nos. 41991251 and 41807442), the Second Tibetan Plateau Scientific Expedition and Research Program (STEP) (Grant No. 2019QZKK0601) and the United States National Natural Science Foundation (Grant Nos. 1648634 and 1648772). We thank Dr. Daniel J. Bain and Miss Yao Zhang for help in the field.

Appendix A. Supplementary data

Supplementary data to this article can be found online at https://doi.org/10.1016/j.scitotenv.2021.146922.

References

- An, Z., Clemens, S.C., Shen, J., Qiang, X., Jin, Z., Sun, Y., Prell, W.L., Luo, J., Wang, S., Xu, H., Cai, Y., Zhou, W., Liu, X., Liu, W., Shi, Z., Yan, L., Xiao, X., Chang, H., Wu, F., Ai, L., Lu, F., 2011. Glacial-interglacial Indian summer monsoon dynamics. Science 333, 719–723. https://doi.org/10.1126/science.1203752.
- An, Z., Wu, G., Li, J., Sun, Y., Liu, Y., Zhou, W., Cai, Y., Duan, A., Li, L., Mao, J., Cheng, H., Shi, Z., Tan, L., Yan, H., Ao, H., Chang, H., Feng, J., 2015. Global monsoon dynamics and climate change. Annu. Rev. Earth Planet. Sc. 43, 29–77. https://doi.org/10.1146/annurevearth-060313-054623.
- Bahrig, B., 1989. Stable isotope composition of siderite as an indicator of the paleoenvironmental history of oil shale lakes. Palaeogeogr. Palaeocl. 70, 139–151. https://doi.org/10.1016/0031-0182(89)90085-0.
- Bai, J., Yang, Z., Cui, B., Gao, H., Ding, Q., 2010. Some heavy metals distribution in wetland soils under different land use types along a typical plateau lake, China. Soil Till. Res. 106, 344–348. https://doi.org/10.1016/j.still.2009.11.003.
- Bai, J., Cui, B., Chen, B., Zhang, K., Deng, W., Gao, H., Xiao, R., 2011. Spatial distribution and ecological risk assessment of heavy metals in surface sediments from a typical plateau lake wetland, China Ecol. Modell. 222, 301–306. https://doi.org/10.1016/j. ecolmodel.2009.12.002.
- Blaauw, M., 2010. Methods and code for "classical" age-modelling of radiocarbon sequences. Quat. Geochronol. 5, 512–518. https://doi.org/10.1016/j.quageo.2010.01.002.
- Bond, G., Showers, W., Cheseby, M., Lotti, R., Almasi, P., DeMenocal, P., Priore, P., Cullen, H., Hajdas, I., Bonani, G., 1997. A pervasive millennial-scale cycle in North Atlantic Holocene and glacial climates. Science 278, 1257–1266. https://doi.org/10.1126/science.278.5341.1257.
- Bond, G., Kromer, B., Beer, J., Muscheler, R., Evans, M.N., Showers, W., Hoffmann, S., Lotti-Bond, R., Hajdas, I., Bonani, G., 2001. Persistent solar influence on North Atlantic climate during the Holocene. Science 294, 2130–2136. https://doi.org/10.1126/science.1065680.
- Briske, D.D., Fuhlendorf, S.D., Smeins, F.E., 2006. A unified framework for assessment and application of ecological thresholds. Rangeland Ecol. Manag. 59, 225–236. https://doi.org/10.2111/05-115R.1.
- Broccoli, A.J., Dahl, K.A., Stouffer, R.J., 2006. Response of the ITCZ to Northern Hemisphere cooling. Geophys. Res. Lett 33, 10–1029. https://doi.org/10.1029/2005GL024546.
- Broecker, W., Bond, G., Klas, M., Clark, E., McManus, J., 1992. Origin of the northern Atlantic's Heinrich events. Clim. Dynam. 6, 265–273. https://doi.org/10.1007/BF00193540.
- Chappuis, E., Seriñá, V., Martí, E., Ballesteros, E., Gacia, E., 2017. Decrypting stable-isotope (δ¹³C and δ¹⁵N) variability in aquatic plants. Freshw. Biol. 62, 1807–1818. https://doi. org/10.1111/fwb.12996.

- Chen, F., Chen, X., Chen, J., Zhou, A., Wu, D., Tang, L., Zhang, X., Huang, X., Yu, J., 2014a. Holocene vegetation history, precipitation changes and Indian Summer Monsoon evolution documented from sediments of Xingyun Lake, south-west China. J. Quaternary Sci. 29, 661–674. https://doi.org/10.1002/jqs.2735.
- Chen, X., Li, Y., Metcalfe, S., Xiao, X., Yang, X., Zhang, E., 2014b. Diatom response to Asian monsoon variability during the Late Glacial to Holocene in a small treeline lake, SW China. Holocene 24, 1369–1377. https://doi.org/10.1177/0959683614540951.
- Chen, F., Xu, Q., Chen, J., Birks, H.J.B., Liu, J., Zhang, S., Jin, L., An, C., Telford, R.J., Cao, X., Wang, Z., Zhang, X., Selvaraj, K., Lu, H., Li, Y., Zheng, Z., Wang, H., Zhou, A., Dong, G., Zhang, J., Huang, X., Bloemendal, J., Rao, Z., 2015. East Asian summer monsoon precipitation variability since the last deglaciation. Sci. Rep. 5, 11186. https://doi.org/10.1038/srep11186.
- Chen, F., Chen, S., Zhang, X., Chen, J., Wang, X., Gowan, E.J., Qiang, M., Dong, G., Wang, Z., Li, Y., Xu, Q., Xu, Y., Smol, J.P., Liu, J., 2020. Asian dust-storm activity dominated by Chinese dynasty changes since 2000 BP. Nat. Commun. 11, 992. https://doi.org/10.1038/s41467-020-14765-4.
- Cheng, Z., Weng, C., Steinke, S., Mohtadi, M., 2018. Anthropogenic modification of vegetated landscapes in southern China from 6,000 years ago. Nat. Geosci. 11, 939–943. https://doi.org/10.1038/s41561-018-0250-1.
- Cheng, N., Liu, L., Hou, Z., Wu, J., Wang, Q., 2020a. Pollution characteristics and risk assessment of surface sediments in nine plateau lakes of Yunnan Province. IOP Conf. Ser.: Earth Environ. Sci. 467, 012166 https://doi.org/10.1088/1755-1315/467/1/012166.
- Cheng, H., Zhang, H., Spötl, C., Baker, J., Sinha, A., Li, H., Bartolomé, M., Moreno, A., Kathayat, G., Zhao, J., Dong, X., Li, Y., Ning, Y., Jia, X., Zong, B., Brahim, Y.A., Pérez-Mejiás, C., Cai, Y., Novello, V.F., Cruz, F.W., Severinghaus, J.P., An, Z., Edwards, R.L., 2020b. Timing and structure of the Younger Dryas event and its underlying climate dynamics. P. Natl. Acad. Sci. USA. 117, 23408–23417. https://doi.org/10.1073/pnas.2007869117
- Chiang, J.C.H., Bitz, C.M., 2005. Influence of high latitude ice cover on the marine Intertropical Convergence Zone. Clim. Dynam. 25, 477–496. https://doi.org/10.1007/ s00382-005-0040-5.
- Clement, A.C., Peterson, L.C., 2008. Mechanisms of abrupt climate change of the last glacial period. Rev. Geophys. 46. https://doi.org/10.1029/2006RG000204.
- Cook, C.G., Jones, R.T., Turney, C.S.M., 2013. Catchment instability and Asian summer monsoon variability during the early Holocene in southwestern China. Boreas. 42, 224–235. https://doi.org/10.1111/j.1502-3885.2012.00287.x.
- Craig, H., 1965. The measurement of oxygen isotope paleotemperatures. In: Tongiorgi, E. (Ed.), Stable Isotopes in Oceanographic Studies and Palae-Otemperatures. Consiglio Nazionale Delle Ricerche Laboratorio di Geologi, Pisa.
- Davison, W., 1993. Iron and manganese in lakes. Earth-Sci. Rev. 34, 119–163. https://doi. org/10.1016/0012-8252(93)90029-7.
- Dean, W.E.J., 1974. Determination of carbonate and organic matter in calcareous sediments and sedimentary rocks by loss on ignition: comparison with other methods. J. Sediment. Res. 44, 242–248. https://doi.org/10.1306/74D729D2-2B21-11D7-8648000102C1865D.
- Dearing, J.A., 2013. Why future earth needs lake sediment studies. J. Paleolimnol. 49, 537–545. https://doi.org/10.1007/s10933-013-9690-1.
- Dearing, J.A., Jones, R.T., Shen, J., Yang, X., Boyle, J.F., Foster, G.C., Crook, D.S., Elvin, M.J.D., 2008. Using multiple archives to understand past and present climate-human-environment interactions: the lake Erhai catchment, Yunnan Province, China. J. Paleolimnol. 40, 3–31. https://doi.org/10.1007/s10933-007-9182-2.
- Denton, G.H., Anderson, R.F., Toggweiler, J.R., Edwards, R.L., Schaefer, J.M., Putnam, A.E., 2010. The last glacial termination. Science 328, 1652–1656. https://doi.org/10.1126/science.1184119.
- Deplazes, G., Lückge, A., Peterson, L.C., Timmermann, A., Hamann, Y., Hughen, K.A., Röhl, U., Laj, C., Cane, M.A., Sigman, D.M., Haug, G.H., 2013. Links between tropical rainfall and North Atlantic climate during the last glacial period. Nat. Geosci. 6, 213–217. https://doi.org/10.1038/ngeo1712.
- Du, H., Chen, Z., Mao, G., Chen, L., Crittenedn, J., Li, R.Y.M., Chai, L., 2019. Evaluation of eutrophication in freshwater lakes: a new non-equilibrium statistical approach. Ecol. Indic. 102, 686–692. https://doi.org/10.1016/j.ecolind.2019.03.032.
- Ekwueme, B.N., Agunwamba, J.C., 2020. Modeling the influence of meteorological variables on runoff in a tropical watershed. Civil Engineering Journal 6, 2344–2351. http://dx.doi.org/10.28991/cej-2020-03091621.
- Fenu, G., Maridina, F., 2020. DSS LANDS: a decision support system for agriculture in Sardinia. HighTech and Innovation Journal 1, 129–135. http://dx.doi.org/10.28991/HIJ-2020-01-03-05.
- Fleitmann, D., Burns, S.J., Mudelsee, M., Neff, U., Kramers, J., Mangini, A., Matter, A., 2003. Holocene forcing of the Indian monsoon recorded in a stalagmite from Southern Oman. Science 300, 1737–1739. https://doi.org/10.1126/science.1083130.
- Goldberg, E.L., Phedorin, M.A., Grachev, M.A., Bobrov, V.A., Dolbnya, I.P., Khlystov, O.M., Levina, O.V., Ziborova, G.A., 2000. Geochemical signals of orbital forcing in the records of palaeoclimates found in the sediments of Lake Baikal. Nucl. Instrum. Meth. A. 448, 384–393. https://doi.org/10.1016/S0168-9002(99)00694-4.
- Goswami, B.N., Ajayamohan, R.S., Xavier, P.K., Sengupta, D., 2003. Clustering of synoptic activity by Indian summer monsoon intraseasonal oscillations. Geophys. Res. Lett. 30, 1431. https://doi.org/10.1029/2002GL016734.
- Govil, P., Divakar Naidu, P., 2011. Variations of Indian monsoon precipitation during the last 32 kyr reflected in the surface hydrography of the Western Bay of Bengal. Quaternary Sci. Rev. 30, 3871–3879. https://doi.org/10.1016/j.quascirev.2011.10.004.
- Gupta, A.K., Anderson, D.M., Overpeck, J.T., 2003. Abrupt changes in the Asian southwest monsoon during the Holocene and their links to the North Atlantic Ocean. Nature 421, 354–357. https://doi.org/10.1038/nature01340.
- Han, T.O., Zin, W.W., Kyi, C., 2020. Analysis of streamflow response to changing climate conditions ssing SWAT model. Civil Engineering Journal 6, 194–209. http://dx.doi. org/10.28991/cej-2020-03091464.

- Heinrich, H., 1988. Origin and consequences of cyclic ice rafting in the Northeast Atlantic Ocean during the past 130,000 years. Quat. Res. 29, 142–152. https://doi.org/10.1016/0033-5894(88)90057-9.
- Hillman, A.L., Abbott, M.B., Yu, J.Q., Steinman, B.A., Bain, D.J., 2016. The isotopic response of Lake Chenghai, SW China, to hydrologic modification from human activity. Holocene 26, 906–916. https://doi.org/10.1177/0959683615622553.
- Hillman, A.L., Abbott, M.B., Finkenbinder, M.S., Yu, J.Q., 2017. An 8,600 year lacustrine record of summer monsoon variability from Yunnan, China. Quaternary Sci. Rev. 174, 120–132. https://doi.org/10.1016/j.quascirev.2017.09.005.
- Hillman, A.L., Abbott, M.B., Yu, J., 2018. Climate and anthropogenic controls on the carbon cycle of Xingyun Lake, China. Palaeogeogr. Palaeocl. 501, 70–81. https://doi.org/ 10.1016/j.palaeo.2018.04.012.
- Hillman, A.L., O'Quinn, R.F., Abbott, M.B., Bain, D.J., 2020. A Holocene history of the Indian monsoon from Qilu Lake, southwestern China. Quaternary Sci. Rev. 227, 106051. https://doi.org/10.1016/j.quascirev.2019.106051.
- Hu, Z. (Ed.), 1999. Atlas of Chinese cultural relics: Yunnan volume, 1st Yunnan Science and Technology Press, Kunming (In Chinese).
- Javadinejad, S., Dara, R., Jafary, F., 2020. Climate change scenarios and effects on snow-melt runoff. Civil Engineering Journal 6, 1715–1725. http://dx.doi.org/10.28991/cej-2020-03091577.
- Jenny, J.P., Koirala, S., Gregory-Eaves, I., Francus, P., Niemann, C., Ahrens, B., Brovkin, V., Baud, A., Ojala, A.E.K., Normandeau, A., Zolitschka, B., Carvalhais, N., 2019. Human and climate global-scale imprint on sediment transfer during the Holocene. P. Natl. Acad. Sci. USA. 116, 22972–22976. https://doi.org/10.1073/pnas.1908179116.
- Jones, R.T., Cook, C.G., Zhang, E., Langdon, P.G., Jordan, J., Turney, C., 2012. Holocene environmental change at Lake Shudu, Yunnan Province, southwestern China. Hydrobiologia 693, 223–235. https://doi.org/10.1007/s10750-012-1124-y.
- Kansoh, R., Abd-El-Mooty, M., Abd-El-Baky, R., 2020. Computing the water budget components for lakes by using meteorological data. Civil Engineering Journal 6, 1255–1265. http://dx.doi.org/10.28991/cej-2020-03091545.
- Keeley, J.E., Sandquist, D.R., 1992. Carbon: freshwater plants. Plant Cell Environ. 15, 1021–1035. https://doi.org/10.1111/j.1365-3040.1992.tb01653.x.
- Kutzbach, J.E., Guetter, P.J., 1986. The influence of changing orbital parameters and surface boundary conditions on climate simulations for the past 18,000 years. J. Atmos. Sci. 43, 1726–1759. https://doi.org/10.1175/1520-0469(1986)0432.0.CO;2.
- Laskar, J., Robutel, P., Joutel, F., Gastineau, M., Correia, A.C.M., Levrard, B., 2004. A long-term numerical solution for the insolation quantities of the Earth. J. Astrophys. Astron. 428, 261–285. https://doi.org/10.1051/0004-6361:20041335.
- Leng, M.J., Marshall, J.D., 2004. Palaeoclimate interpretation of stable isotope data from lake sediment archives. Quaternary Sci. Rev. 23, 811–831. https://doi.org/10.1016/j. guascirev.2003.06.012.
- Li, K., 2004. A summary of the main achievements of the mankind origin study and the prehistoric archaeology in Yunnan. Social Science in Yunnan 2, 108–113. https:// doi.org/10.3969/j.issn.1000-8691.2004.02.025.
- Li, Y., Qiang, M., Wang, G., Li, F., Liu, Y., Jin, Y., Li, H., Jin, M., 2015. Processes of exogenous detrital input to Genggahai Lake and climatic changes in the Gonghe basin since the Late Glacial. Quaternary Sciences 35, 160–171. https://doi.org/10.11928/j.issn.1001-7410.2015.01.15.
- Li, K., Tan, B., Ni, J., Liao, M., 2018a. Hydroclimate changes since Last Glacial Maximum: geochemical evidence from Yilong Lake, southwestern China. Acta Ecol. Sin. 38, 8973–8982. https://doi.org/10.5846/stxb201806011228.
- Li, Y., Chen, X., Xiao, X., Zhang, H., Xue, B., Shen, J., Zhang, E., 2018b. Diatom-based inference of Asian monsoon precipitation from a volcanic lake in southwest China for the last 18.5 ka. Quaternary Sci. Rev. 182, 109–120. https://doi.org/10.1016/j.guascirev.2017.11.021.
- Liu, X., Wang, H., 2016. Dianchi Lake, China: geological formation, causes of eutrophication and recent restoration efforts. Aquat. Ecosyst. Health 19, 40–48. https://doi.org/10.1080/14634988.2016.1145022.
- Liu, Y., Zhang, W., Wang, Y., 1979. Chinese fauna of economic animals: Freshwater *Mollusca*, first ed. Science Press, Beijing. (In Chinese).
- Liu, X., Ning, P., Zhang, J., Chen, J., Yang, F., Zhang, X., 2006. Towards the effects of reclaiming the land from the lake and restoring the lake from the land in Yilong Lake. Journal of Kunming University of Science and Technology (Science and Technology). 31, pp. 79–81 (In Chinese with English abstract).
- Liu, E., Shen, J., Zhang, E., Wu, Y., Yang, L., 2010. A geochemical record of recent anthropogenic nutrient loading and enhanced productivity in Lake Nansihu, China. J. Paleolimnol. 44, 15–24. https://doi.org/10.1007/s10933-009-9382-z.
- Liu, X., Liu, J., Chen, S., Chen, J., Zhang, X., Yan, J., Chen, F., 2020. New insights on Chinese cave δ^{18} O records and their paleoclimatic significance. Earth-Sci. Rev. 207, 103216. https://doi.org/10.1016/j.earscirev.2020.103216.
- MacDonald, G.M., Beukens, R.P., Kieser, W.E., Vitt, D.H., 1987. Comparative radiocarbon dating of terrestrial plant macrofossils and aquatic moss from the 'ice-free corridor' of western Canada. Geology 15, 837–840. https://doi.org/10.1130/0091-7613(1987) 152.0.CO;2.
- Mackereth, F.J.H., 1966. Some chemical observations on post-glacial Lake sediments. Phil. Trans. R. Soc. Lod. B. 250, 165–213. https://doi.org/10.1098/rstb.1966.0001.
- Maher, B.A., 2008. Holocene variability of the East Asian summer monsoon from Chinese cave records: a re-assessment. Holocene 18, 861–866. https://doi.org/10.1177/0959683608095569.
- Mckenzie, J.A., Hollander, D.J., 1993. Oxygen-isotope record in recent carbonate sediments from Lake Greifen, Switzerland (1750–1986): Application of continental isotopic indicator for evaluation of changes in climate and atmospheric circulation patterns. , pp. 101–111 https://doi.org/10.1029/gm078p0101.
- Menviel, L., Timmermann, A., Mouchet, A., Timm, O., 2008. Meridional reorganizations of marine and terrestrial productivity during Heinrich events. Paleoceanography 23, A1203. https://doi.org/10.1029/2007PA001445.

- Meyers, P.A., 1994. Preservation of elemental and isotopic source identification of sedimentary organic matter. Chem. Geol. 114, 289–302. https://doi.org/10.1016/0009-2541(94)90059-0.
- Meyers, P.A., 1997. Organic geochemical proxies of paleoceanographic. Org. Geochem. 27, 213–250. https://doi.org/10.1016/S0146-6380(97)00049-1.
- Moreno, A., López-Merino, L., Leira, M., Marco-Barba, J., González-Sampériz, P., Valero-Garcés, B.L., López-Sáez, J.A., Santos, L., Mata, P., Ito, E., 2011. Revealing the last 13,500 years of environmental history from the multiproxy record of a mountain lake (Lago Enol, northern Iberian Peninsula). J. Paleolimnol. 46, 327–349. https://doi.org/10.1007/s10933-009-9387-7.
- Mozley, P.S., Wersin, P., 1992. Isotopic composition of siderite as an indicator of depositional environment. Geology 20, 817–820. https://doi.org/10.1130/0091-7613 (1992)0202.3.CO:2.
- Neff, U., Burns, S.J., Mangini, A., Mudelsee, M., Fleitmann, D., Matter, A., 2001. Strong coherence between solar variability and the monsoon in Oman between 9 and 6 kyr ago. Nature 411, 290–293. https://doi.org/10.1038/35077048.
- Nelson, D.B., Abbott, M.B., Steinman, B., Polissar, P.J., Stansell, N.D., Ortiz, J.D., Rosenmeier, M.F., Finney, B.P., Riedel, J., 2011. Drought variability in the Pacific Northwest from a 6,000-yr lake sediment record. P. Natl. Acad. Sci. USA. 108, 3870–3875. https://doi.org/10.1073/pnas.1009194108.
- O'Beirne, M.D., Werne, J.P., Hecky, R.E., Johnson, T.C., Katsev, S., Reavie, E.D., 2017. Anthropogenic climate change has altered primary productivity in Lake Superior. Nat. Commun. 8, 15713. https://doi.org/10.1038/ncomms15713.
- Olsson, I., 1986. Radiometric methods. In: Berglund, B. (Ed.), Handbook of Holocene Palaeoecology and Palaeohydrology. John Wiley and Sons, Chichester, pp. 273–312.
- O'Reilly, C.M., Alin, S.R., Plisnier, P.D., Cohen, A.S., McKee, B.A., 2003. Climate change decreases aquatic ecosystem productivity of Lake Tanganyika, Africa. Nature 424, 766–768. https://doi.org/10.1038/nature01833.
- Prell, W.L., Kutzbach, J.E., 1992. Sensitivity of the Indian monsoon to forcing parameters and implications for its evolution. Nature 360, 647–652. https://doi.org/10.1038/ 360647a0.
- Rasmussen, S.O., Vinther, B.M., Clausen, H.B., Andersen, K.K., 2007. Early Holocene climate oscillations recorded in three Greenland ice cores. Quaternary Sci. Rev. 26, 1907–1914. https://doi.org/10.1016/j.quascirev.2007.06.015.
- Reimer, P.J., Austin, W.E.N., Bard, E., Bayliss, A., Blackwell, P.G., Bronk Ramsey, C., Butzin, M., Cheng, H., Edwards, R.L., Friedrich, M., Grootes, P.M., Guilderson, T.P., Hajdas, I., Heaton, T.J., Hogg, A.G., Hughen, K.A., Kromer, B., Manning, S.W., Muscheler, R., Palmer, J.G., Pearson, C., van der Plicht, J., Reimer, R.W., Richards, D.A., Scott, E.M., Southon, J.R., Turney, C.S.M., Wacker, L., Adolphi, F., Büntgen, U., Capano, M., Fahrni, S.M., Fogtmann-Schulz, A., Friedrich, R., Köhler, P., Kudsk, S., Miyake, F., Olsen, J., Reinig, F., Sakamoto, M., Sookdeo, A., Talamo, S., 2020. The IntCal20 northern hemisphere radiocarbon age calibration curve (0–55 cal kBP). Radiocarbon 62, 725–757. https://doi.org/10.1017/rdc.2020.41.
- Shakun, J.D., Carlson, A.E., 2010. A global perspective on Last Glacial Maximum to Holocene climate change. Quaternary Sci. Rev. 29, 1801–1816. https://doi.org/10.1016/j.quascirev.2010.03.016.
- Shen, J., 2009. Progress and prospect of palaeolimnology research in China. J. Lake Sci. 21, 307–313. https://doi.org/10.18307/2009.0301.
- Shen, J., Yang, L., Yang, X., Matsumoto, R., Tong, G., Zhu, Y., Zhang, Z., Wang, S., 2005. Lake sediment records on climate change and human activities since the Holocene in Erhai catchment, Yunnan Province, China. Sci. China Ser. D. 48, 353–363. https://doi.org/ 10.1360/03vd0118.
- Singer, C., Shulmeister, J., McLea, B., 1998. Evidence against a significant Younger Dryas cooling event in New Zealand. Science 281, 812–814. https://10.1126/ science.281.5378.812.
- Song, X., Yao, Y., Wortley, A.H., Paudayal, K.N., Yang, S., Li, C., Blackmore, S., 2012. Holocene vegetation and climate history at Haligu on the Jade Dragon Snow Mountain, Yunnan, SW China. Clim. Chang. 113, 841–866. https://doi.org/10.1007/s10584-011-0364-6.
- Stringham, T.K., Krueger, W.C., Shaver, P.L., 2003. State and transition modeling: An ecological process approach. J. Range Manag 56, 106–113. https://doi.org/10.2307/4003893, 2003.
- Sun, W., Jiang, Q., Liu, E., Chang, J., Zhang, E., 2018. Climate change dominates recent sedimentation and organic carbon burial in Lake Chenghai, southwest China. J. Limnol. 77. https://doi.org/10.4081/jlimnol.2018.1762.
- Sun, Y., Liu, S., Shi, F., An, Y., Li, M., Liu, Y., 2020. Spatio-temporal variations and coupling of human activity intensity and ecosystem services based on the four-quadrant model on the Qinghai-Tibet Plateau. Sci. Total Environ. 743, 140721. https://doi.org/ 10.1016/j.scitotenv.2020.140721.
- Tan, M., 2014. Circulation effect: response of precipitation δ^{18} O to the ENSO cycle in monsoon regions of China. Clim. Dynam. 42, 1067–1077. https://doi.org/10.1007/s00382-013-1732-x.
- Tanaka, K., Akagawa, F., Yamamoto, K., Tani, Y., Kawabe, I., Kawai, T., 2007. Rare earth element geochemistry of Lake Baikal sediment: its implication for geochemical response to climate change during the Last Glacial/Interglacial transition. Quaternary Sci. Rev. 26, 1362–1368. https://doi.org/10.1016/j.quascirev.2007.02.004.
- Tomas, R.A., Webster, P.J., 1997. The role of inertial instability in determining the location and strength of near-equatorial convection. Q. J. Roy. Meteor. Soc. 123, 1445–1482. https://doi.org/10.1002/qj.49712354202.
- Walker, B., Meyers, J.A., 2004. Thresholds in ecological and social-ecological systems. Ecol. Soc. 9, 3. https://doi.org/10.5751/ES-00664-090203.
- Wang, S., Dou, H., 1998. Lakes in China. 1st. Science Press, Beijing (In Chinese).

- Wang, P., Clemens, S., Beaufort, L., Braconnot, P., Ganssen, G., Jian, Z., Kershaw, P., Sarnthein, M., 2005a. Evolution and variability of the Asian monsoon system: state of the art and outstanding issues. Quaternary Sci. Rev. 24, 595–629. https://doi.org/ 10.1016/j.guascirev.2004.10.002
- Wang, Y., Cheng, H., Edwards, R.L., He, Y., Kong, X., An, Z., Wu, J., Kelly, M.J., Dykoski, C.A., Li, X., 2005b. The Holocene Asian monsoon: links to solar changes and North Atlantic climate. Science 308, 854–857. https://doi.org/10.1126/science.1106296.
- Wang, Q., Yang, X., Anderson, N.J., Dong, X., 2016. Direct versus indirect climate controls on Holocene diatom assemblages in a sub-tropical deep, alpine lake (Lugu Hu, Yunnan, SW China). Quat. Res. 86, 1–12. https://doi.org/10.1016/j.yqres.2016.03.003.
- Wang, P., Wang, B., Cheng, H., Fasullo, J., Guo, Z., Kiefer, T., Liu, Z., 2017. The global monsoon across time scales: mechanisms and outstanding issues. Earth-Sci. Rev. 174, 84–121. https://doi.org/10.1016/j.earscirev.2017.07.006.
- Waters, C.N., Zalasiewicz, J., Summerhayes, C., Barnosky, A.D., Poirier, C., Gałuszka, A., Cearreta, A., Edgeworth, M., Ellis, E.C., Ellis, M., Jeandel, C., Leinfelder, R., McNeill, J.R., Richter, D.D.B., Steffen, W., Syvitski, J., Vidas, D., Wagreich, M., Williams, M., Zhisheng, A., Grinevald, J., Odada, E., Oreskes, N., Wolfe, A.P., 2016. The Anthropocene is functionally and stratigraphically distinct from the Holocene. Science 351, 137–147. https://doi.org/10.1126/science.aad2622.
- Webster, P.J., Magaña, V.O., Palmer, T.N., Shukla, J., Tomas, R.A., Yanai, M., Yasunari, T., 1998. Monsoons: processes, predictability, and the prospects for prediction. J. Geophys. Res. 103, 14451–14510. https://doi.org/10.1029/97jc02719.
- Wei, K., Gasse, F., 1999. Oxygen isotopes in lacustrine carbonates of West China revisited: implications for post glacial changes in summer monsoon circulation. Quaternary Sci. Rev. 18, 1315–1334. https://doi.org/10.1016/S0277-3791(98)00115-2.
- Weltje, G.J., Tjallingii, R., 2008. Calibration of XRF core scanners for quantitative geochemical logging of sediment cores: theory and application. Earth Planet. Sc. Lett. 274, 423–438. https://doi.org/10.1016/j.epsl.2008.07.054.
- Wen, Z., Zheng, H., Ouyang, Z., 2020. Research progress on the relationship between biodiversity and ecosystem services. Chin. J. Appl. Ecol. 31, 340–348. https://doi.org/ 10.13287/j.1001-9332.202001.003.
- Wolfe, B.B., Edwards, T.W.D., Aravena, R., 1999. Changes in carbon and nitrogen cycling during tree-line retreat recorded in the isotopic content of lacustrine organic matter, western Taimyr Peninsula, Russia. Holocene 9, 215–222. https://doi.org/10.1191/ 095968399669823431.
- Wu, D., Zhou, A., Liu, J., Chen, X., Wei, H., Sun, H., Yu, J., Bloemendal, J., Chen, F., 2015a. Changing intensity of human activity over the last 2,000 years recorded by the magnetic characteristics of sediments from Xingyun Lake, Yunnan, China. J. Paleolimnol. 53, 47–60. https://doi.org/10.1007/s10933-014-9806-2.
- Wu, D., Zhou, A., Chen, X., Yu, J., Zhang, J., Sun, H., 2015b. Hydrological and ecosystem response to abrupt changes in the Indian monsoon during the last glacial, as recorded by sediments from Xingyun Lake, Yunnan, China. Palaeogeogr. Palaeocl. 421, 15–23. https://doi.org/10.1016/j.palaeo.2015.01.005.
- Wu, D., Chen, X., Lv, F., Brenner, M., Curtis, J., Zhou, A., Chen, J., Abbott, M., Yu, J., Chen, F., 2018. Decoupled early Holocene summer temperature and monsoon precipitation in southwest China. Quaternary Sci. Rev. 193, 54–67. https://doi.org/10.1016/j. quascirev.2018.05.038.
- Xiao, X., Haberle, S.G., Li, Y., Liu, E., Shen, J., Zhang, E., Yin, J., Wang, S., 2018. Evidence of Holocene climatic change and human impact in northwestern Yunnan Province: high-resolution pollen and charcoal records from Chenghai Lake, southwestern China. Holocene 28, 127–139. https://doi.org/10.1177/0959683617715692.
- Xie, Y. (Ed.), 1984. Atlas of Quartz Sand Surface Textural Features of China Micrographs, 1st China Ocean Press, Beijing.
- Xu, H., Goldsmith, Y., Lan, J., Tan, L., Wang, X., Zhou, X., Cheng, J., Lang, Y., Liu, C., 2020. Juxtaposition of Western Pacific subtropical high on Asian summer monsoon shapes subtropical east Asian precipitation. Geophys. Res. Lett. 47, e2019GL084705. doi: https://doi.org/10.1029/2019GL084705.
- Yu, S., Colman, S.M., Lowell, T.V., Milne, G.A., Fisher, T.G., Breckenridge, A., Boyd, M., Teller, J.T., 2010. Freshwater outburst from Lake Superior as a trigger for the cold event 9300 years ago. Science 328, 1262–1266. https://doi.org/10.1126/science.1187860.
- Zhai, H., Cui, B., Zhao, X., Liu, S., Hu, B., Yao, M., 2006. Spatial variability and distribution of soil nutrient contents along different environmental gradients of Yilong lake shore. Acta Ecol. Sin 26, 61–69 (In Chinese with English abstract).
- Zhang, E., Liu, E., Shen, J., Cao, Y., Li, Y., 2012. One century sedimentary record of lead and zinc pollution in Yangzong Lake, a highland lake in southwestern China. J. Environ. Sci. 24, 1189–1196. https://doi.org/10.1016/S1001-0742(11)60896-6.
- Zhang, E., Sun, W., Ji, M., Zhao, C., Xue, B., Shen, J., 2015. Late Quaternary carbon cycling responses to environmental change revealed by multi-proxy analyses of a sediment core from an upland lake in southwest China. Quat. Res. 84, 415–422. https://doi. org/10.1016/j.yqres.2015.09.004.
- Zhang, E., Chang, J., Shulmeister, J., Langdon, P., Sun, W., Cao, Y., Yang, X., Shen, J., 2019. Summer temperature fluctuations in Southwestern China during the end of the LGM and the last deglaciation. Earth Planet. Sc. Lett. 509, 78–87. https://doi.org/ 10.1016/j.epsl.2018.12.024.
- Zhao, L., Wang, M., Liang, Z., Zhou, Q., 2020. Identification of regime shifts and their potential drivers in the shallow eutrophic Lake Yilong, Southwest China. Sustainability 2020, 12. doi:https://doi.org/10.3390/su12093704.
- Zhou, A., He, Y., Wu, D., Zhang, X., Zhang, C., Liu, Z., Yu, J., 2015. Changes in the Radiocarbon Reservoir Age in Lake Xingyun, Southwestern China during the Holocene. PLoS One 10, e0121532. https://doi.org/10.1371/journal.pone.0121532.